ELSEVIER

Cretaceous Research 29 (2008) 373–385

CRETACEOUS RESEARCH

www.elsevier.com/locate/CretRes

Geochemical characterization of bentonite beds in the Two Medicine Formation (Campanian, Montana), including a new $^{40}Ar/^{39}Ar$ age

B.Z. Foreman [a,*], R.R. Rogers [a], A.L. Deino [b], K.R. Wirth [a], J.T. Thole [a]

[a] *Department of Geology, Macalester College, St. Paul, MN 55105, USA*
[b] *Berkeley Geochronology Center, Berkeley, CA 94709, USA*

Received 26 July 2007; accepted in revised form 31 July 2007
Available online 7 August 2007

Abstract

Terrestrial deposits of the Upper Cretaceous (Campanian) Two Medicine Formation of northwestern Montana preserve multiple bentonite beds ($n \geq 19$) that reflect recurrent pyroclastic events in the Western Interior Basin. Major and trace element concentrations were determined on 27 samples derived from four bentonites using X-ray fluorescence spectroscopy. This study evaluates the potential for geochemically distinguishing three of these bentonite beds using a stepwise discriminant analysis of trace element concentrations. Seven elements were found sufficient to establish 100% classification in the group matrix. The elements (in order of decreasing contribution to the canonical discriminant functions) are Zr, Sc, V, Cr, U, Ga, and Th. The validity of these results is strongly supported by cross-validation methods that correctly assigned 100% of randomly-selected bentonite samples left out of the stepwise analysis to their correct bed. These findings indicate geochemical discrimination is a viable tool for correlation within the formation and suggests its application to more distant coeval strata. We also report here a new $^{40}Ar/^{39}Ar$ age of 77.52 ± 0.19 Ma for one of the analyzed bentonite beds. This new radioisotopic age affords insights into the timing of regional eruptive events, and further constrains the age of the Two Medicine Formation and its renowned fossil resources. Finally, the inferred magmatic composition of the original ash (based on trace element compositions) from the two older bentonites beds suggest a source in the Elkhorn Mountain Volcanics whereas the younger bentonites may have been sourced from the Adel Mountain Volcanics.

Keywords: Late cretaceous; Montana; Stratigraphy; Bentonite; Geochemistry; Radioisotopic dating

1. Introduction

Geochemical discrimination of altered volcanic ash beds (bentonites) allows for long distance correlation across facies boundaries and therefore serves as a powerful tool for the stratigraphic analysis of sedimentary basins. For example, Randle et al. (1971) discriminated ash fall deposits from the Cascade Range using geochemical ternary and bivariate plots, supplemented with petrographic analyses, and correlated the ash beds ~115 km from their source. In a longer ranging study of considerably older marine deposits, Kolata et al. (1986) used a stepwise discriminant analysis to geochemically discriminate and correlate four bentonite horizons across ~900 km in the Ordovician Decorah Subgroup in the upper Mississippi valley region. More recently, Thomas et al. (1990) distinguished the Campanian-aged Plateau Tuff in Dinosaur Provincial Park in Alberta, Canada, from related bentonite horizons using unique compositions of plagioclase populations as well as principal component analysis and factor analysis of whole-rock elemental concentrations. These studies and others (e.g., Lerbekmo, 1968; Jack and Carmichael, 1969; Borchardt et al., 1971; Huff, 1983; Delano and Tice, 1993; Wray, 1999; Christidis, 2001; Pellenard et al., 2003) exemplify potential approaches to geochemical discrimination and correlation of bentonite horizons, and illustrate the power and utility of this method.

This study seeks to evaluate the viability of the geochemical method for Two Medicine Formation bentonite beds and

* Corresponding author. Present address: Department of Geological Sciences, University of Michigan, 2534 C. C. Little Building, 1100 North University Ave, Ann Arbor, MI 48109, USA.
E-mail address: bforema1@uwyo.edu (B.Z. Foreman).

0195-6671/$ - see front matter
doi:10.1016/j.cretres.2007.07.001

employs an approach outlined by Huff and Kolata (1989) and used by Kolata et al. (1986), Huff (1983), and Pellenard et al. (2003). In this approach multiple samples are derived from laterally-persistent bentonite beds and their whole-rock trace element concentrations submitted to a stepwise discriminant analysis. Samples from each distinct bentonite bed are treated as a group and element concentrations as variables. The multivariate statistical analysis then weights and linearly combines the variables to optimize statistical differences. The resulting canonical functions can be used to assign bentonite samples of unknown origin to their source bed. It should also be noted that despite group membership being known *a priori*, the stepwise discriminant analysis will not necessarily assign samples to the correct group (bed) if geochemical differences are not sufficient. Moreover, the cross-validation method, leaving select samples out of the discriminant analysis, can be used to evaluate the success of the resulting canonical functions to assign "unknown" samples to the correct group (bed).

In our application of this method the three bentonite beds entered into the analysis could be distinguished using seven elements (Zr, Sc, V, Cr, U, Ga, and Th). The cross-validation method, repeated for each of the samples of the three bentonites included in the analysis, correctly assigned 100% of samples to their source bentonite bed. These results show that the bentonites are geochemically distinct and indicate the geochemical method is a viable tool for correlation among bentonite beds within the Two Medicine Formation. In addition to the geochemical discrimination of the Two Medicine bentonite beds, we report a new $^{40}Ar/^{39}Ar$ age (77.52 ± 0.19 Ma) for one of the targeted bentonite horizons that is located approximately 265 m above the base of the formation. This new radioisotopic date provides additional age control for the Two Medicine Formation and its included paleofauna.

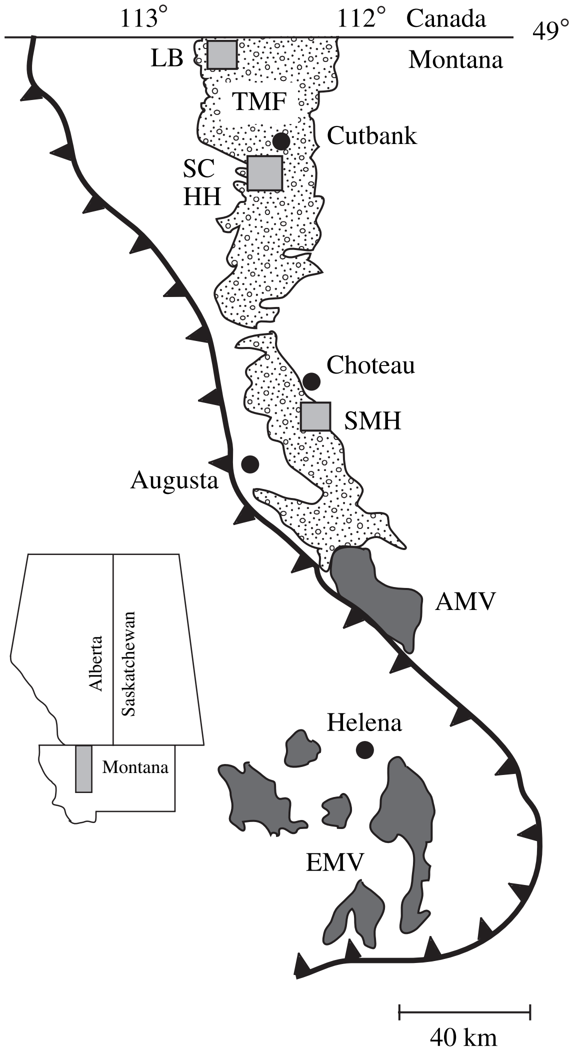

Fig. 1. Map showing Two Medicine Formation (TMF), Elkhorn Mountain Volcanics (EMV), and Adel Mountain Volcanics (AMV) exposures in northwestern Montana, and sample localities at Seven Mile Hill (SMH), Shield's Crossing (SC), Hadro Hill (HH), and Landslide Butte (LB) (modified from Ross et al., 1955; Viele and Harris, 1965; Rogers, 1998).

2. Two Medicine Formation

The Upper Cretaceous (Campanian) Two Medicine Formation consists predominantly of terrestrial deposits that accumulated along the western margin of the Western Interior Seaway during two major third-order sea-level cycles (Rogers, 1998) (Fig. 1). The unit reaches a thickness of ~550 m and is dominated by fine- to medium-grained sandstone bodies, variegated mudstones, and siltstones derived from the Cordilleran highlands and the Elkhorn Mountain Volcanics. Strata of the Two Medicine Formation are correlative with upper horizons of the Eagle Formation and the Judith River Formation in central Montana, both of which accumulated in nearshore marine and nonmarine environments. Marine equivalents within Montana include the Claggett Formation and the lower part of the Bearpaw Formation (Stebinger, 1914; Gill and Cobban, 1973; Rogers et al., 1993). In Alberta, equivalent strata include the marine Pakowki, Milk River, and Bearpaw formations, and terrestrial beds of the Belly River and Judith River groups (Russell, 1970; McLean, 1971; Goodwin and Deino, 1989; Eberth and Hamblin, 1993). In Wyoming and Utah parts of the Mesa Verde and Kaiparowits Formations, respectively, are terrestrial equivalents of the Two Medicine Formation (Sanderson, 1931; Roberts et al., 2005). These formations contain numerous bentonite beds that are at least coeval with, if not derived from the same eruptions recorded in the Two Medicine Formation. The Two Medicine Formation is ideal for this study as it alone contains at least 19 individual bentonite beds, spans most of the Campanian stage, and represents the most proximal record of sedimentation in Montana at that time (Rogers, 1995).

Bentonites throughout the Two Medicine Formation range in color from olive-gray (5Y-5/2) to yellow (10YR-7/6), typically exhibit prominent popcorn weathering texture, form topographic benches on outcrops, and have sharp basal contacts and sharp to gradational upper contacts (Table 1). Euhedral biotite and plagioclase phenocrysts are common near basal contacts. Smectite is the predominant clay mineral (Rogers, 1990; this study, unpublished results). The altered ash horizons vary in thickness from a few centimeters to over two meters, and many show significant lateral variation

Table 1
Location, ages, stratigraphy, and sedimentologic descriptions of bentonite beds in this study from the Two Medicine Formation

Bentonite Horizon	Location	Number of Samples Collected	Stratigraphy	Age	Sedimentologic characteristics
Seven Mile Hill (SMH)	sec. 27, T23N, R5W, Seven Mile Hill N47°42'53" W112°13'43"	9	~80 m above base of Two Medicine Formation	79.72 ± 0.03 Ma (SE) plagioclase[a] 79.77 ± 0.11 Ma (SE) biotite[a]	olive-gray (5Y-5/2) bentonite, 30–175 cm thick, lateral variation, lower contact sharp, biotite phenocrysts present upper contact sharp to gradational, overlies pink plagioclase crystal tuff, popcorn weathering texture, authigenic limonite and present
Shield's Crossing (SC)	sec. 2,T31N, R6W, Rock City N48°28'33" W112°20'54"	2	~100 m above the base of Two Medicine Formation	79.60 ± 0.1 Ma (SE) plagioclase[a]	yellow (10YR-7/6) bentonite. 10–25 cm thick, lateral variation, biotite present under handlens, lower and upper contacts sharp, interbedded with carbonaceous shales, overlies vertebrate microfossil bonebed, popcorn weathering
Hadro Hill (HH)	sec. 15, T31N, R7W Flag Butte N48°27'12" W112°29'59"	4	~265 m above the base of Two Medicine Formation	77.52 ± 0.2 Ma (SE) sanidine[b]	greenish-gray (GLEY-6/1) bentonite, ~170 cm thick, biotite present, lower contact sharp, upper contact sharp to gradational, overlies dark grey siltstone with abundant gastropod fossils, authigenic limonite and selenite present
Landslide Butte (LB)	sec. 22, T37N, R20W, Landslide Butte N48°55'59" W112°39'08"	12	~505 m above the top of Two Medicine Formation	not dated	dark gray (10YR-4/1) to greenish brown bentonite, 55–125 cm, lateral variation, lower contact sharp, upper contact gradational, abundant biotite present throughout, feldspar present under handlens, popcorn weathering texture, authigenic limonite present

[a] Rogers et al., 1993.
[b] this study.

in thickness. Bentonite beds of the Two Medicine Formation commonly overlie carbonaceous lacustrine deposits, paleosol sequences, overbank mudstones, and fluvial channel sandstones (Rogers et al., 1993; King, 1997; Roberts, 1999; Roberts and Hendrix, 2000). The material erupted during lava flows, ignimbrites, and ashfalls had a significant impact on terrestrial depositional systems forming volcaniclastic "aprons" and introducing volcanically produced debris and hyper-concentrated flows into fluvial systems (King, 1997; Smith, 1998; Smith and Schmitt, 1998). Moreover, Two Medicine Formation sedimentary strata interfinger with volcanic deposits of the Elkhorn Mountain Volcanics which were active throughout the Campanian (Viele and Harris, 1965; Chadwick, 1981; Rogers et al., 1993; King, 1997). The Adel Mountains Volcanics (AMV), located ~60 km south of Two Medicine Formation outcrops near Choteau, MT, is another possible source for bentonites and volcaniclastics younger than ~76 Ma. The AMV are notably more mafic in composition than the Elkhorn Mountain Volcanics (Harlan et al., 1991; Cunningham, 1999) (Fig. 1).

This study focuses on four bentonites located at 1) Seven Mile Hill (SMH), 2) Shield's Crossing (SC), 3) Hadro Hill (HH), and 4) Landslide Butte (LB) (Fig. 1, Table 1). The bentonites are located at various stratigraphic positions within the Two Medicine Formation (Fig. 2). The Seven Mile Hill bentonite was dated by Rogers et al. (1993, their TM-3 bentonite) using $^{40}Ar/^{39}Ar$ methods, and yielded a radioisotopic age of 79.72 ± 0.03 Ma (plagioclase). The Shield's Crossing bentonite is intercalated in a bentonite-rich interval along the Two Medicine River and was dated by Rogers et al. (1993) at 79.60 ± 0.1 Ma (plagioclase). These nearly contemporaneous bentonite beds have been used to date and correlate a proposed nonmarine sequence boundary, the lower discontinuity (LD) of Rogers (1994; 1998), with an unconformity in marine rocks associated with the Ardmore bentonite sequence of similar age. The Hadro Hill bentonite is dated herein at 77.52 ± 0.19 Ma (sanidine). This bentonite is located approximately 65 m below the upper discontinuity of Rogers (1994; 1998). This discontinuity is marked by an abrupt shift in alluvial architecture to finer-grained facies and lacustrine deposition and is possibly equivalent to the onset of the Bearpaw transgression ~75 Ma. The Landslide Butte bentonite has not been radioisotopically dated, but it is stratigraphically higher and thus younger than the TM-4 bentonite, dated by Rogers et al. (1993) at 74.3 ± 0.2 Ma. The Landslide Butte bentonite bed has previously served as a local datum for the correlation of proposed drought-related death assemblages of ceratopsians and hadrosaurs (Rogers, 1990).

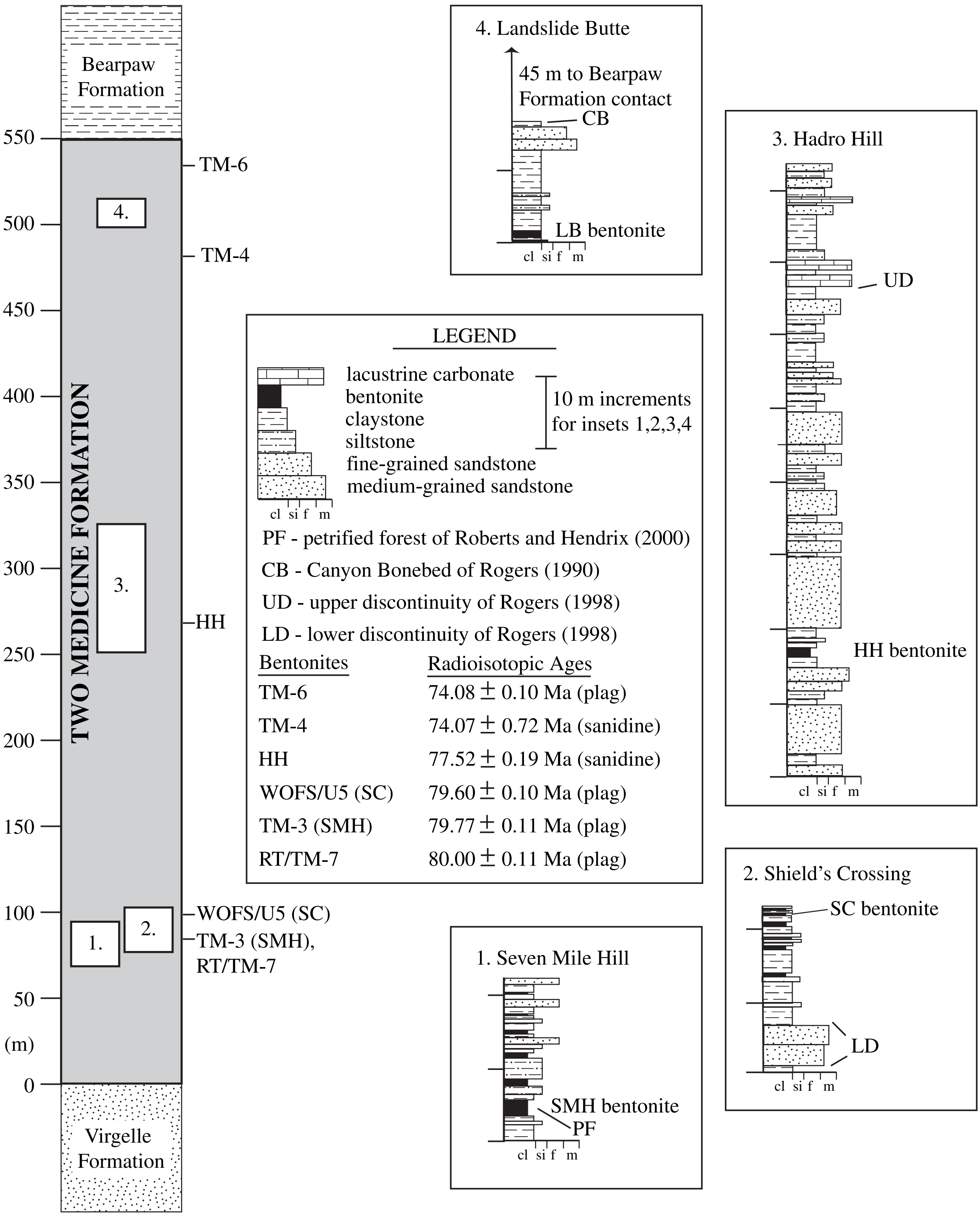

Fig. 2. Stratigraphic distribution of previous dated bentonites in the Two Medicine Formation (Rogers et al., 1993), bentonites of this study, representative stratigraphic sections of sample sites, and notable paleoenvironmental and sequence stratigraphic features. Sections drafted and modified from Rogers (1990; 1995; 1998).

3. Materials and methods

3.1. Sample localities

Bentonite horizons were physically ‘‘walked-out’’ along exposures and sampled laterally. The Seven Mile Hill and Landslide Butte bentonites were sampled laterally across approximately 10 km of exposure. Lateral sampling of the Hadro Hill and Shield's Crossing bentonites was limited to approximately ~1 km and ~30 m, respectively, due to less exposure. The Seven Mile Hill (SMH), Hadro Hill (HH), and Landslide Butte (LB) bentonites were sampled twice at each locality, once immediately above the basal contact (e.g. SMH1-b), and again ~40 cm above the basal contact (e.g. SMH1-m). The Shield's Crossing bentonite (SC) was sampled only at the base due to its limited thickness ($\leq$ 25 cm). In all cases, outcrop localities were trenched to expose fresh material for sampling. In total, 27 samples were collected: SMH ($n = 9$), LB ($n = 12$), HH ($n = 4$), and SC ($n = 2$).

3.2. XRF methods

Bentonite samples were analyzed for major and trace element concentrations using a Philips PW2400 X-ray Fluorescence Spectrometer (XRF) housed at Macalester College. Major and trace element concentrations were determined on fused beads and pressed pellets, respectively. Sample preparation and analytical techniques followed those described in detail by Vervoort et al. (in press) using the same XRF. A tungsten-carbide shatterbox was used to pulverize samples for fused beads, and a case-hardened mild steel shatterbox was used for powder pellets. Two replicate analyses were performed per bead and pellet, the averages of which represent the reported element concentrations. Element concentrations were calibrated against U.S. Geological Survey standards (soil USGS SO-3, soil USGS GXR-2), other international certified reference materials (Bedford dolerite GeoPT4/OU-2, Mount Hood Andesite GeoPT5/AMH-1), and internal standards (rhyolite RSTDA-1, basalt HB-74). The percentage difference between determined concentrations of standards and their published values was larger than that between replicate bentonite analyses. Element concentrations from the bentonite beds are above the limits of detections calculated by Vervoort et al. (in press) for the XRF spectrometer at Macalester College. The reported relative analytical uncertainties, the percentage difference between analyzed standards and their published values, are <0.5% for major element concentrations and <3% for trace element concentrations, except for U, which was ~8%. These errors differ from those reported by Vervoort et al. (in press), but are preferred because they were analyzed at the same time as the bentonite samples.

3.3. Statistical methods

Trace element concentrations from the Seven Mile Hill, Hadro Hill, and Landslide Butte bentonite beds were submitted to a step-wise discriminant analysis following the methods outlined by Huff and Kolata (1989) using the Statistical Package for the Social Sciences (SPSS ver. 11). Each of the three bentonite beds was considered a group to which the individual samples belong. The 11 trace elements are treated as variables that are thought to differ among the groups. The multivariate stepwise discriminant analysis weights and linearly combines multiple variables in an attempt to achieve maximum separation (discrimination) among the groups. The Wilks' lambda method was used to obtain the optimal ranking of variables (elements). Trace element concentrations are chosen for inclusion into the step-wise analysis if the element's probability of F ratio (the ratio of the mean between-group variance to the mean within-group variance) is less than 0.05. A ‘‘probability of F for removal’’ of 0.10 was used. The process continues, selecting the next best discriminator until additional variables cannot add significant discriminating power (i.e. the remaining variables all have significance values greater than 0.05 or 100% discrimination among the groups has already been achieved). The result is a set of coefficients that define a linear canonical discriminant function, the maximum number of functions is equal to one less than the number of groups or the number of independent variables whichever is smaller (Klecka, 1981).

3.4. $^{40}Ar/^{39}Ar$ dating methods

Feldspar phenocrysts obtained for $^{40}Ar/^{39}Ar$ dating were separated from samples of the Hadro Hill bentonite. Bulk samples were disaggregated in H_2O_2 and tap water, and sieved through 20, 40, 60, and 100 mesh screens. The resulting relatively crystal-rich fractions were ultrasonically cleaned in distilled water for 10 minutes, and feldspars concentrated using a Frantz isodynamic separator. Handpicked euhedral to subhedral feldspars were then treated in dilute 0.7% hydrofluoric acid for 5 minutes in an ultrasonic cleaner to remove any remaining clay.

Crystal concentrates were loaded into wells in an aluminum disk, and irradiated for 200 hours in the Cd-lined, in-core CLICIT facility at the Oregon State University TRIGA reactor. Fish Canyon Tuff sanidine from Colorado was used as a mineral standard, with a reference age of 28.02 Ma (Renne et al., 1998). $^{40}Ar/^{39}Ar$ analyses were performed at the Berkeley Geochronology Center using a CO_2 laser to rapidly melt individual crystals under ultra-high vacuum. After a 3-minute cleanup on SAES getters, the argon gas liberated from the feldspars in this total-fusion experiment was measured for 30 minutes on a MAP 215-50 mass spectrometer.

4. Results

4.1. Stepwise discriminant analysis

Whole-rock geochemical compositions are reported in Table 2. Multivariate discriminant analysis is necessary for this type of geochemical data set as no single elemental concentration is able to distinguish the four bentonite beds examined in this study. For example, uranium concentrations are

Table 2
Analytical data from XRF analyses of 27 bentonite samples form the Two Medicine Formation

	SMH1-b	SMH1-m	SMH2-b	SMH2-m	SMH5-b	SMH5-m	SMH6-b	SMH6-m	SMH-m	SC1-b	SC2-b
Oxides (wt %)											
SiO_2	58.29	58.78	60.62	60.53	62.15	60.99	60.07	60.87	58.72	55.73	68.55
Al_2O_3	20.57	20.33	18.96	19.25	18.52	19.06	20.33	20.22	20.11	22.39	14.93
TiO_2	0.52	0.54	0.49	0.50	0.47	0.49	0.52	0.52	0.52	0.73	0.60
Fe_2O_3	5.30	5.33	4.34	5.19	4.32	4.63	4.09	4.07	5.44	5.31	4.26
MnO	0.01	0.01	0.02	0.01	0.01	0.01	0.01	0.01	0.01	0.01	0.02
MgO	3.58	3.66	3.25	3.58	3.35	3.74	3.33	3.51	4.07	3.10	1.70
CaO	1.21	1.12	1.60	1.07	1.31	1.37	1.37	0.90	0.74	1.68	0.39
Na_2O	2.79	2.74	3.09	2.97	2.43	2.53	2.74	3.06	3.20	2.66	1.61
K_2O	0.45	0.42	0.52	0.28	0.33	0.25	0.38	0.27	0.38	1.07	3.10
P_2O_5	0.06	0.07	0.07	0.07	0.05	0.07	0.08	0.06	0.07	0.15	0.14
LOI	7.02	6.76	6.62	6.26	6.68	6.69	6.87	6.15	6.58	6.02	3.72
Total	99.80	99.76	99.58	99.71	99.62	99.83	99.79	99.64	99.84	98.85	99.03
Trace elements (ppm)											
Ba	260	240	1090	160	610	300	530	260	230	290	290
Ce	178	178	123	166	142	156	185	182	159	63	62
Co	5.5	3.8	4.9	4.3	5.7	3.5	5.8	4.7	3.9	4.1	4.9
Cr	5.2	5.6	5.4	5.4	5.1	6.1	5.0	5.2	5.8	3.5	3.8
Ga	21.4	21.5	18.1	20.8	20.0	20.6	21.0	21.2	21.8	22.6	23.5
La	120	120	80	112	93	104	126	124	106	56	58
Nb	19.4	21.8	17.2	22.6	18.0	24.1	15.0	21.7	24.9	20.4	19.3
Ni	11.3	8.8	10.2	8.4	11.7	5.9	9.9	7.6	6.7	15.7	15.6
Pb	31.2	32.4	32.0	32.8	30.3	36.8	33.3	39.5	37.1	34.2	36.7
Rb	18.7	14.7	26.3	10.7	16.6	9.3	17.0	12.7	14.7	34.9	35.0
Sc	11.2	10.9	10.0	9.8	10.6	10.7	11.0	10.4	10.9	10.8	11.4
Sr	290	245	989	217	881	426	962	322	206	323	324
Th	24.9	24.2	20.8	23.3	22.5	22.7	24.0	23.8	24.5	23.2	25.2
U	6.9	7.1	6.3	7.8	6.2	7.7	8.6	7.4	7.6	3.2	3.7
V	42	38	33	30	37	39	39	47	38	39	39
Y	36.5	37.1	32.8	35.7	35.9	33.0	44.1	42.2	33.2	30.3	30.0
Zn	74	723	57	68	73	66	68	66	73	112	112
Zr	424	420	375	398	388	401	389	411	425	407	408

	HH1-b	HH1-m	HH2-b	HH2-m	LB1-b	LB1-m	LB2-b	LB2-m	LB3-b	LB3-m
Oxides (wt %)										
SiO_2	61.82	67.14	62.08	66.05	71.84	59.05	59.09	58.90	59.03	58.33
Al_2O_3	18.03	15.87	18.03	16.65	13.45	19.93	19.53	18.78	19.59	19.29
TiO_2	0.21	0.27	0.21	0.29	0.51	0.29	0.30	0.34	0.36	0.31
Fe_2O_3	4.55	3.10	4.51	3.22	3.23	4.78	4.56	5.13	4.84	5.45
MnO	0.01	0.01	0.01	0.01	0.01	0.01	0.02	0.02	0.02	0.01
MgO	4.35	3.73	4.63	3.80	1.59	3.93	3.98	4.14	3.88	4.51
CaO	1.13	1.12	0.65	0.85	0.77	1.54	1.53	1.69	1.52	1.10
Na_2O	3.06	2.43	3.55	2.59	1.89	3.19	3.06	2.86	3.54	3.35
K_2O	0.36	0.65	0.40	0.97	2.65	0.85	0.91	1.02	1.22	0.88
P_2O_5	0.05	0.06	0.05	0.06	0.12	0.09	0.09	0.06	0.10	0.09
LOI	6.03	5.36	5.56	5.14	3.04	5.78	6.12	6.26	5.13	5.88
Total	99.60	99.74	99.68	99.63	99.10	99.44	99.19	99.20	99.23	99.20
Trace elements (ppm)										
Ba	170	240	160	260	630	622	620	870	580	430
Ce	75	68	80	98	52	50	50	56	58	47
Co	5.6	3.9	4.0	4.3	10.9	9.1	9.2	10.7	8.1	9.8
Cr	2.9	10.3	3.4	13.4	48.2	8.4	6.8	12.6	8.4	11.1
Ga	20.1	18.3	20.3	19.0	18.2	24.0	24.5	24.4	23.0	23.9
La	44	40	49	61	32	40	40	47	50	46
Nb	22.8	20.6	22.8	20.8	17.6	25.2	25.1	24.5	24.1	26.8
Ni	9.9	6.9	8.8	8.0	18.8	17.2	16.9	17.4	19.0	18.0
Pb	30.1	26.4	28.9	26.4	21.7	31.8	33.4	24.1	29.4	28.8
Rb	7.4	25.7	9.1	38.5	117.3	25.5	25.3	33.4	37.5	29.3
Sc	3.7	5.3	3.4	5.7	9.2	7.4	7.3	8.2	7.7	7.4
Sr	188	147	127	155	183	358	358	437	253	209

Table 2 (*continued*)

	HH1-b	HH1-m	HH2-b	HH2-m	LB1-b	LB1-m	LB2-b	LB2-m	LB3-b	LB3-m
Th	26.3	24.7	26.6	25.7	8.9	29.7	29.0	25.1	28.3	32.1
U	10.6	9.9	11.9	10.5	3.6	7.9	7.2	6.5	6.5	9.8
V	15	31	14	40	85	16	17	27	20	15
Y	7.6	15.7	8.5	20.9	30.6	23.4	23.7	23.7	25.4	26.0
Zn	52	46	51	43	81	62	62	66	67	70
Zr	139	129	138	132	185	194	193	189	191	184

	LB4-b	LB4-m	LB5-b	LB5-m	LB6-b	LB6-m
Oxides (wt %)						
SiO_2	65.48	62.36	59.62	58.12	57.39	59.84
Al_2O_3	16.73	17.72	19.53	19.17	19.00	18.75
TiO_2	0.42	0.36	0.34	0.30	0.31	0.31
Fe_2O_3	3.84	4.59	4.47	4.85	5.40	5.67
MnO	0.01	0.01	0.02	0.02	0.02	0.02
MgO	2.80	3.64	3.69	4.12	4.33	4.23
CaO	1.16	1.12	1.63	1.62	1.27	1.28
Na_2O	2.72	2.71	3.14	3.13	3.03	2.83
K_2O	1.68	1.35	1.11	0.94	0.87	0.83
P_2O_5	0.09	0.07	0.11	0.09	0.08	0.03
LOI	4.25	5.21	5.38	7.02	7.92	5.65
Total	99.18	99.14	99.04	99.38	99.62	99.44
Trace elements (ppm)						
Ba	570	360	2750	390	840	180
Ce	56	48	53	56	32	61
Co	9.6	8.3	8.9	10.6	10.6	13.2
Cr	24.0	20.5	10.2	7.3	7.4	15.5
Ga	21.3	21.8	20.8	24.2	23.8	24.6
La	40	40	41	49	26	55
Nb	22.5	20.8	17.8	25.6	26.5	24.6
Ni	19.2	18.1	19.7	15.9	16.1	22.9
Pb	23.2	26.4	29.3	31.0	28.0	23.7
Rb	64.3	52.7	30.9	26.7	24.1	33.5
Sc	8.2	8.1	7.2	7.4	7.3	8.7
Sr	228	217	472	464	331	394
Th	20.5	23.4	24.9	27.6	29.6	22.1
U	6.2	6.5	4.4	6.4	8.9	8.8
V	50	36	22	17	18	30
Y	25.1	24.0	21.4	27.2	17.6	25.9
Zn	72	60	82	66	61	66
Zr	199	181	215	193	189	152

able to distinguish the SMH, SC, and HH bentonite beds from one another, but none can be distinguished from the LB bentonite bed (Fig. 3A). Similarly the LB and HH bentonite can be distinguished from the SC and SMH bentonite beds using zirconium concentrations, but SMH and SC concentrations overlap (Fig. 3B). At least two bentonite beds overlap (intervals determined from two standard deviations from the mean) for every element analyzed. The multivariate discriminant analysis approach allows for the consideration of many elements simultaneously to obtain a more useful and rigorous distinction among the bentonite beds.

The step-wise discriminant analysis was performed on the SMH, HH, and LB bentonite beds (SC did not have adequate sample numbers). Chromium, Ga, La, Nb, Pb, Sc, Th, U, V, Y, and Zr were initially entered in the analysis. These elements are generally regarded as stable under diagenetic processes (Borchardt et al., 1971; Randle et al., 1971; Winchester and Floyd, 1977; Christidis, 1998). The step-wise analysis yielded two discriminant functions, and seven elements were sufficient for discrimination among the three beds. These elements are (in order of decreasing contribution to the discriminant function) Zr, Sc, V, Cr, U, Ga, and Th. The statistical properties of these discriminant functions are presented in Table 2. The eigenvalues shown are a measure of the relative amount of variance among the groups for which the elements can account for (Table 2). The corresponding percent of variance shows that the first discriminant function accounts for 93.7% of the variance and the second discriminant function accounts for the remaining 6.3% of variance. In both functions the canonical correlation coefficients are quite high 0.998 and 0.978, indicating they are effective bentonite discriminators. Unstandardized weighting coefficients for each of the elements in the canonical discriminant functions are presented in Table 2. Individual bentonite samples can be related to group means (centroids) on a territorial map by entering elemental concentrations for each sample into the canonical discriminant

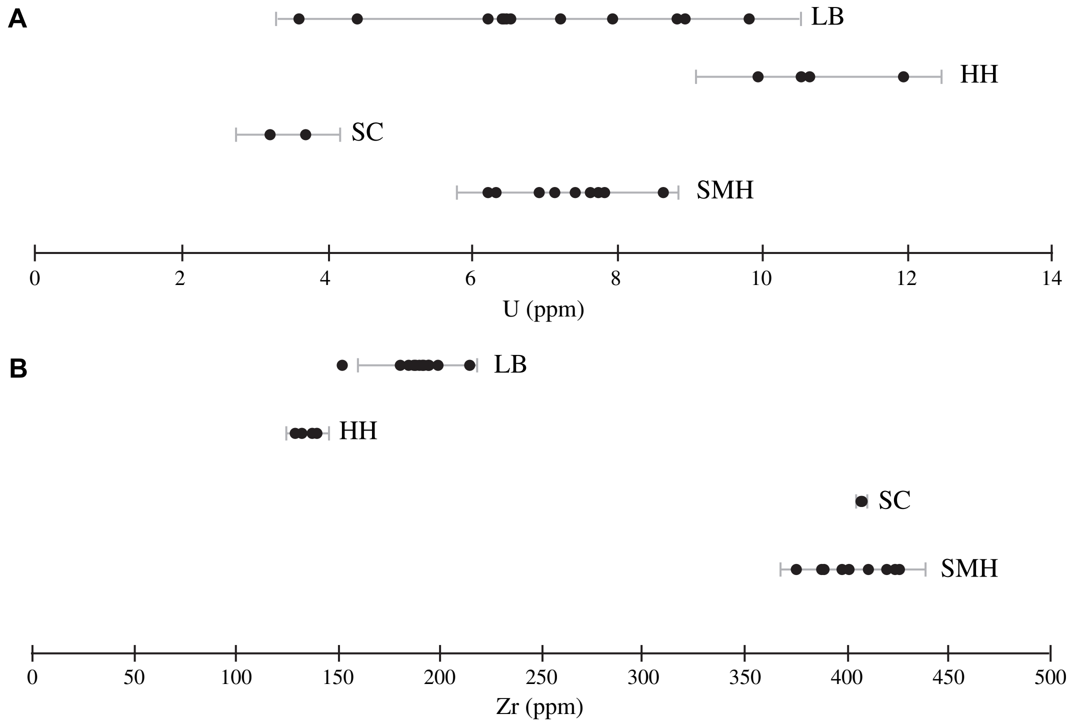

Fig. 3. A, Uranium concentrations for four analyzed bentonites B, Zirconium concentrations for four analyzed bentonites. Gray bars represent two standard deviations from the mean.

functions (Fig. 4). SMH, HH, and LB samples plot near their respective group centroid, with no overlap (Fig. 4). Thus, the discriminant functions are 100% successful at distinguishing the three bentonite beds from one another. In order to assess the robustness of the discriminant functions cross-validation methods were used. The stepwise discriminant analysis was repeated 25 times, each time leaving out a single, randomly-selected sample. After the analysis the resulting discriminant functions were used to classify the removed sample. The sample was assigned to the correct bentonite bed 100% of the time (Table 3).

4.2. $^{40}Ar/^{39}Ar$ dating results

Results from the $^{40}Ar/^{39}Ar$ dating effort are summarized in Table 4. A total of 37 single-crystal, total-fusion $^{40}Ar/^{39}Ar$ ages were obtained from phenocrystic feldspar separated from the Hadro Hill bentonite, 32 from plagioclase and the remaining five from sanidine. The sanidine grains form a fairly simple, sharply defined age-probability distribution ranging in age from 76.6 to 77.8 (Fig. 5) with a weighted mean of 77.52 ± 0.19 Ma (1σ). All demonstrate the high proportion of radiogenic argon to total ^{40}Ar ('% $^{40}Ar^*$') expected for sanidines of this age (>98%). The mean sum of weighted deviates (MSWD) indicates all observed scatter can be explained by analytical uncertainty. We interpret the sanidine age as the geological (eruptive) age for this unit. The plagioclase analyses also form a simple, gaussian-like age distribution, but due to lower potassium concentration, individual ages are more than an order of magnitude less precise than those of the sanidine. Three plagioclase analyses yielded anomalously young ages (Fig. 5) and relatively low %$^{40}Ar^*$ (Table 4). These probably represent altered or inclusion-rich material. Excluding these, the weighted mean age for the plagioclase population is 75.8 ± 0.7 Ma, statistically indistinguishable from the sanidine mean at a 95% confidence interval.

The new sanidine $^{40}Ar/^{39}Ar$ age of 77.52 ± 0.19 from the Two Medicine Formation type area is compatible with the existing radioisotopic framework, based on $^{40}Ar/^{39}Ar$ analyses of underlying and overlying bentonite horizons (Rogers et al., 1993). The Hadro Hill (HH) bentonite is ~160 m above the Shields Crossing (SC) bentonite, situated within a thin interval of closely-spaced bentonites that has yielded an age of 79.6 ± 0.2 Ma (SE) (see WOFS-U5 in Rogers et al., 1993), and ~215 m below the TM-4 bentonite, which yielded an age of 74.3 Ma $\pm$ 0.2 Ma (SE) (Rogers et al., 1993).

5. Discussion

5.1. Implications for Two Medicine Formation stratigraphy

This study successfully uses a stepwise discriminant analysis approach to characterize of Two Medicine Formation bentonites, and represents the first attempt to do so in this richly fossiliferous and volcaniclastic formation. The four bentonite horizons studied here represent at least three and potentially four distinct stratigraphic horizons within the ~550 m thick Two Medicine Formation.

The discriminant analysis method is sensitive to variations in geochemical concentrations and is able to identify and combine the most significant of those variations in order to

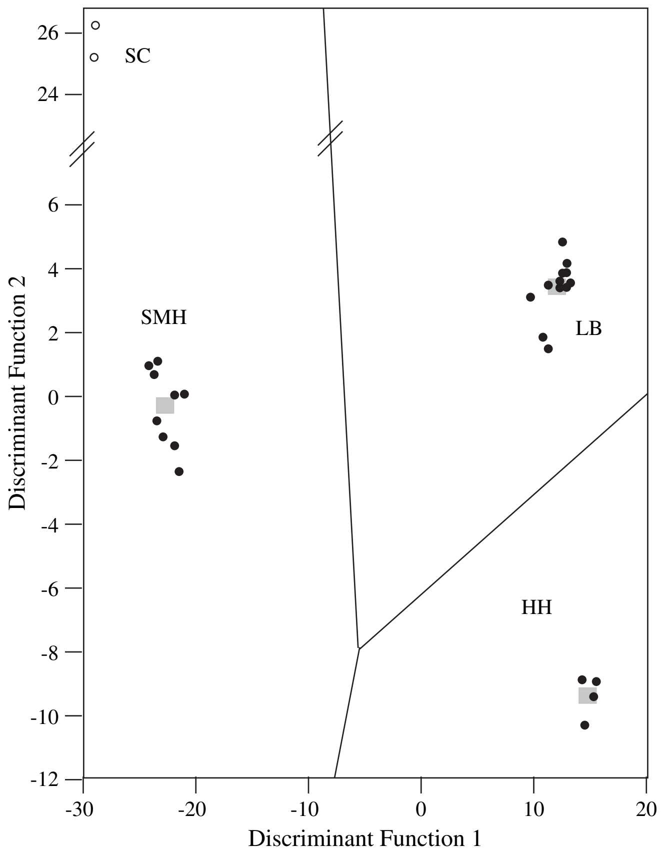

Fig. 4. Territorial map utilizing canonical discrimination functions from seven immobile trace elements (Zr, Sc, V, Cr, U, Ga, and Th). Gray squares mark the group centroids and the filled circles represent bentonite samples (SMH\, HH, and LB). SC (open circles) were not included in the statistical analysis, but were plotted based upon the generated discriminant functions.

distinguish the beds. Moreover, by plotting unknown bentonite samples using the calculated discriminant functions one can confirm bentonite correlations based on other methods or suggest new possible correlations (Huff, 1983; Huff and Kolata, 1989). In addition, new bentonite horizons can be added to the framework by recalculating the step-wise discriminant analysis with new whole-rock data. For example, the addition of Ardmore bentonite analyses from the Bearpaw Formation may confirm that one of the Ardmore bentonite beds represents the distal marine equivalent of the Seven Mile Hill bentonite. This bodes well for future stratigraphic studies both within the Two Medicine Formation and between this formation and correlative units. This method of correlation, however, first necessitates analyses of multiple bentonite samples that can be correlated laterally (i.e. walked out) to establish the geochemical uniqueness of the horizon, prior to its extension to bentonites of unknown stratigraphic position. The high degree of reproducibility and correct classification, based on reduced sample sizes during the cross-validation methods strongly argues for the robustness of the geochemical ‘‘fingerprints’’.

Geochemical differences among bentonites are caused by either different eruptive sources or magma chamber evolution that alters chemical composition prior to an eruptive phase. The overlapping radioisotopic ages of the SMH and SC bentonite beds, which are separated by ~85 km, suggest that they may represent a single widespread volcanic ash fall. Indeed, Roberts and Hendrix (2000) linked the Seven Mile Hill bentonite in Montana with the Ardmore bentonite succession in the Dakotas and Nebraska based on age and mineralogic similarities (Hicks et al., 1995; Bertog and Huff, 1999; Hicks et al., 1999), and it is certainly possible that this same major eruption also sent ash to the north to form the SC bentonite. The diminishing thickness trend between SMH (~150 cm) and SC (~20 cm) is consistent with the hypothesis of a single, large pyroclastic eruption that thins distally from the Elkhorn Mountain Volcanics source area. It is equally plausible, however, that the two bentonite beds are the products of two discrete eruptive events from contemporaneous eruptions of different sources or eruptions from the same source but at times within the error of the radioisotopic method. When immobile trace element concentrations from two Shields Crossing bentonite bed samples were entered into the generated discriminant functions they plot within the field of the Seven Mile Hill bentonite, but away from the SMH group centroid (Fig. 4). This result suggests that the bentonite beds do not represent the same eruptive event. However, it is possible that the Shield's Crossing bentonite was derived from the same source as the Seven Mile Hill bentonite that had undergone some degree of magmatic evolution between eruptions. However, the possibility that lateral variations chemical composition may be cause of this result cannot entirely be ruled out, but this possibility is thought to be less likely. The lateral chemical consistency found in the SMH and LB bentonites, within their study areas, over 10 km despite variations in thickness typically on the order of half a meter or more argues against lateral chemical variability being the cause of SC and SMH differences. Our results suggest that geochemical correlations linked with radioisotopic ages allow for the construction of more highly refined stratigraphic frameworks than those frameworks based upon radioisotopic ages alone.

This method holds significant potential for high-resolution correlation among coeval strata, the refining of proposed ‘‘dinosaurian faunas’’ (Horner et al., 2001), and an independent framework in which to test nonmarine sequence stratigraphic correlations (Rogers, 1998). Furthermore, bentonites of similar age crop out in both nonmarine and marine formations in Canada, other parts of Montana, the Dakotas, Nebraska, Wyoming, and Utah (Spivey, 1940; Gill and Cobban, 1973; Thomas et al., 1990; Eberth and Deino, 1992; Eberth and Hamblin, 1993; Rogers, 1998; Bertog and Huff, 1999; Roberts et al., 2005). This research represents the initial attempt to create a highly-resolved geochemical stratigraphic framework for the Campanian of the Western Interior. Within this proposed framework more regional questions regarding sedimentation patterns, sea-level fluctuations, paleoclimate, and paleobiology can be posed with temporal meaning.

5.2. Age of the Two Medicine Formation

All radioisotopic age data reported for the Two Medicine Formation (Rogers et al., 1993; present study) are consistent

Table 3
Discriminant function properties for SMH, HH, and LB bentonites

Discriminant Function Properties				
Function	Eigenvalue	Percent of Variance	Cumulative percentage	Canonical correlation
1	120.11	87.3	87.3	0.996
2	17.522	12.7	100	0.973
Discriminant functions evaluated at group means				
Bentonite	Function 1	Function 2		
SMH	14.252	−1.016		
HH	−11.115	−7.657		
LB	−5.797	3.23		
Unstandardized discriminant function coefficients				
Element	Function 1	Function 2		
Sc	1.076	1.196		
Ga	−0.218	1.048		
Zr	0.086	0.004		
La	−0.027	−0.084		
U	0.6	−0.671		
Constant	−28.417	−22.628		

with the unit accumulating during most of the Campanian Stage (83.5–70.6 Ma, Gradstein et al., 2004), with deposition definitively commencing prior to 80 Ma and terminating shortly after 74 Ma. The new radioisotopic age reported herein for the Hadro Hill (HH) bentonite of 77.52 ± 0.19 Ma is significant because it serves to further constrain the age of the ''dinosaurian faunas'' of Horner et al. (2001), which have been described as having potential biostratigraphic utility. The HH bentonite is intercalated in the Two Medicine Formation type area near the top of Horner et al's. (2001) ''Lithofacies 3,'' which includes the ''*Gryposaurus latidens* Biozone.''

The new age reported here for the HH bentonite is also important from a basin analysis perspective, because it serves to constrain the timing of a major reorganization of depositional systems in the Two Medicine type area. Rogers (1998) described an abrupt and widespread shift from fluvial and floodplain deposits to lacustrine carbonate facies ~330 m above the base of the formation. The ''anomalous'' lacustrine carbonate interval, which spans ~55 m, was tentatively linked to increased accommodation (subsidence) in the proximal foreland basin. The HH bentonite crops out ~65 m below the lacustrine deposits in the type area, and thus serves to place a lower limit on the timing of this major depositional systems reorganization.

5.3. *Source of Two Medicine Formation bentonites*

The abundant volcaniclastic detritus and bentonite horizons found in the Two Medicine Formation have commonly been attributed to the Elkhorn Mountain Volcanics (EMV) (Viele and Harris, 1965; Chadwick, 1981; Lorenz, 1981; Rogers et al., 1993, 1998; King, 1997; Roberts and Hendrix, 2000). The ~1500 m thick EMV consist of andesitic flows, breccias, tuffs, and rhyolitic ash-flow tuffs located in the area around Wolf Creek and Helena, Montana (Fig. 1) (Chadwick, 1981). Smedes (1966) identified pyroclastic and epiclastic volcanic rocks in the EMV with rhyolitic, rhyodactic, andesitic, and basaltic compositions. Thomas et al. (1990) also linked the EMV to the Campanian-aged Plateau Tuff and related bentonites in southern Alberta. In their study, Thomas et al. (1990) showed that the geochemical composition of the Plateau Tuff is consistent with parent magma compositions ranging from rhyodacite to dacite. Tilling et al. (1968) reported ages between 74 Ma to 83 Ma for the EMV. The Adel Mountain Volcanics (AMV) contains trachybasalt and trachyandesite lava flows and sills, among intrusive volcanics such as syenogabbro dikes, latite and quartz latite lava flows (Lyons, 1944). Harlan et al. (1991) estimated the base of the AMV to be ~76 Ma based on $^{40}Ar/^{39}Ar$ whole-rock ages.

Geochemical data derived from Two Medicine bentonites that relate to magma composition is consistent with eruption from both the EMV and AMV. The discrimination diagram of Winchester and Floyd (1977) was used to estimate original magma composition of the altered ash beds (Fig. 6). Seven Mile Hill bentonite samples fall predominantly in the rhyolitic and rhyodacitic fields with a few samples on the division with trachyandesite. The Shield's Crossing bentonite samples border rhyodacitic/dacitic and trachyandesitic compositions. Eleven of the twelve Landslide Butte bentonite samples lie within the trachyandesite field. Hadro Hill bentonite samples lie within both trachyandesite and trachyte. Andesitic to rhyodacitic/dacite compositions dominate EMV deposits (Chadwick, 1981), and compare favorably to compositions determined herein for Seven Mile Hill and Shield's Crossing bentonites. Moreover, the interpreted erupted ages for the two bentonites (~80 Ma) fall within the age constraints of EMV eruptive events, and EMV lava flows and tuffs interfinger with southern exposures of Two Medicine Formation (Viele and Harris, 1965; Chadwick, 1981; Rogers et al., 1993; King, 1997). The Landslide Butte and Hadro Hill bentonites are more mafic than the Seven Mile Hill and Shield's Crossing bentonites, and have compositions more similar to those found in the AMV than the EMV. The age of the Landslide Butte bentonite is younger than the lower constraints on AMV eruptions, but the Hadro Hill bentonite is slightly older (by ~1.5 Ma) than the oldest dated AMV deposits (~76 Ma). However, the composition of these bentonite beds is consistent with an AMV source.

6. Conclusions

This study establishes the suitability of geochemical discrimination for bentonites in the Two Medicine Formation,

Table 4
Analytical data for $^{40}Ar/^{39}Ar$ analyses from Hadro Hill bentonite sanidine and plagioclase crystals. (Lab ID #22641, Irradiation 31 b ($J = 5.262 \pm 0.001 \times 10^{-4}$)

Material	Ca/K	±1σ	$^{40}Ar^*/^{39}Ar$	±1σ	Age (Ma)	±1σ	MSWD	Prob.	n/n_{total}
Sanidine	0.0046	0.0007	0.8338	0.0014	77.52	0.19	1.76	0.13	5/5
Plagioclase	8.896	0.017	0.816	0.008	75.8	0.7	1.25	0.17	29/32

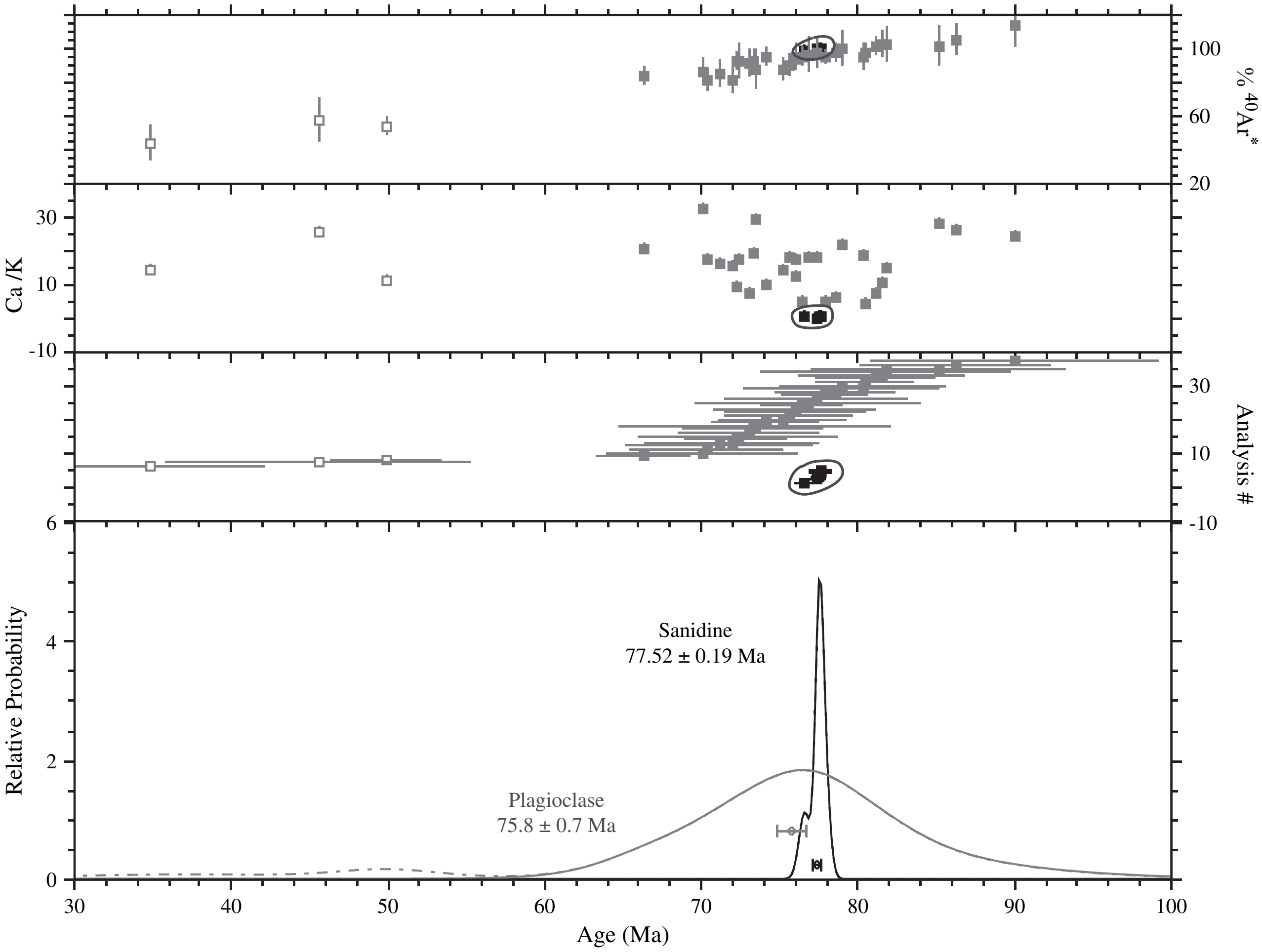

Fig. 5. Age-probability spectra for Hadro Hill bentonite. Circled data points are sanidine analyses. The three outliers are the likely altered or inclusion-rich plagioclase crystals.

and presents a new $^{40}Ar/^{39}Ar$ radioisotopic age for a bentonite horizon intercalated approximately in the middle of the formation in the type area along the Two Medicine River. A stepwise discriminant analysis of immobile trace element concentrations from three discrete bentonite beds identified the most discriminating elements are Zr, Sc, V, Cr, U, Ga, and Th. The resulting canonical discriminant functions proved successful at classifying 100% of unknown samples using the cross-validation method. The unstandardized canonical functions can be utilized in future studies to support stratigraphic correlations. Moreover, this research can be extended to include more bentonite beds from the formation. The stepwise discriminant analysis results also suggest that the Seven Mile Hill and Shields Crossing bentonite beds may represent different eruptive events that occurred coevally, or two events erupted from different sources. Given the suitability of Two Medicine bentonites to geochemical ‘‘fingerprinting,’’ the stage is now set for the establishment of a highly-refined tephrostratigraphic framework both within the Two Medicine Formation (which includes at least 19 discrete bentonite beds) and between the Two Medicine Formation and contemporaneous units in the Western Interior Basin. The generation of an independent stratigraphic framework founded on geochemical

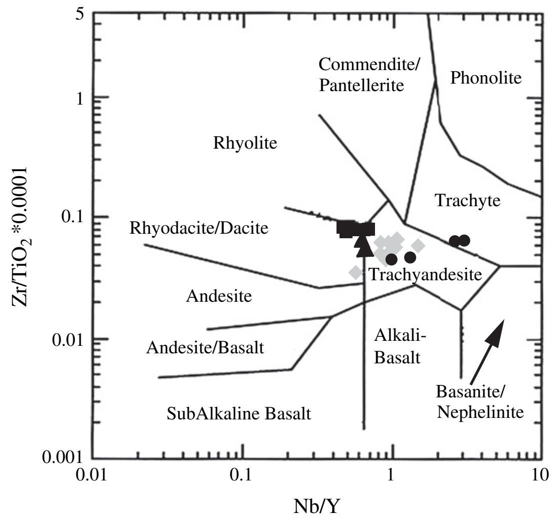

Fig. 6. Discrimination diagram after Winchester and Floyd (1977) showing original magmatic composition of the unaltered bentonites. SMH samples are represented with squares, SC with triangles, HH with circles, and LB with diamonds.

correlations will permit the testing of existing sequence stratigraphic reconstructions (e.g., Rogers, 1998), and enhance the potential to study paleobiological phenomena (e.g., Horner et al., 1992, 2001) in a meaningful chronostratigraphic framework. Finally, our findings suggest the Seven Mile Hill and Shield's Crossing bentonite beds were derived from the Elkhorn Mountain Volcanics and that the Hadro Hill and Landslide Butte bentonites were derived from the Adel Mountain Volcanics.

Acknowledgements

This study was financially supported by research grants from Macalester College (Keck Faculty-Student Collaboration Grant, Beltmann Student Research Grant), the Minnesota NASA Space Grant Consortium Scholarship, and whole-rock chemical analyses were supported by National Science Foundation grants (DUE-9452255, EAR-9601475, DUE-9651385, and EAR-0520870) to Macalester College. We wish to thank R. Hanna, M. Brady, C. Dwyer, and M. D'Emic for field assistance, as well as S. Stevens, R. Wellman, and R. Reagan for land access. We also thank M. Hendrix and D. Eberth for their constructive reviews.

References

Bertog, J.L., Huff, W.D., 1999. Biotite geochemistry of the bentonites in the Sharon Springs member of the Pierre Shale (Campanian, Late Cretaceous): their use in magmatic interpretation and stratigraphic correlation. Abstracts with Programs. Geological Society of America 31, 233.

Borchardt, G.A., Harward, M.E., Schmitt, R.A., 1971. Correlation of volcanic ash deposits by activation analysis of glass separates. Quaternary Research 1, 247–260.

Chadwick, R.A., 1981. Chronology and structural setting of volcanism in southwestern and central Montana. In: Tucker, T.A. (Ed.), Southwest Montana, pp. 301–310 (Montana Geology Society, Field Conference 1981).

Christidis, G.E., 1998. Comparative study of the mobility of major and trace elements during alteration of an andesite and a rhyolite to bentonite, in the islands of Milos and Kimolos, Aegean, Greece. Clays and Clay Minerals 46, 379–399.

Christidis, G.E., 2001. Geochemical correlation of bentonites from Milos Island, Aegean, Greece. Clay Minerals 36, 295–306.

Cunningham, B., 1999. Petrogenesis of the Adel Mountains Volcanic Field, central Montana, Unpublished Maters thesis, Department of Geology, University of Montana, Missoula, 82 pp.

Delano, J.W., Tice, S., 1993. Geochemical fingerprinting of volcanic glass from K-bentonites in the Utica Shale and Trenton Group, New York State: Stratigraphic and structural implications. Abstracts with Programs. Geological Society of America 25, 33.

Eberth, D.A., Deino, A.L., 1992. A geochronology of the nonmarine Judith River Formation of southern Alberta. SEPM Theme Meeting, Mesozoic of the Western Interior, 24–25.

Eberth, D.A., Hamblin, A.P., 1993. Tectonic, stratigraphic, and sedimentologic significance of a regional discontinuity in the upper Judith River Group (Belly River wedge) of southern Alberta, Saskatchewan, and northern Montana. Canadian Journal of Earth Sciences 30, 174–200.

Gill, J.R., Cobban, W.A., 1973. Stratigraphy and geologic history of the Montana Group and equivalent rocks, Montana, Wyoming, and North and South Dakota. United States Geological Survey, Professional Paper 776, 37.

Goodwin, M.B., Deino, A.L., 1989. The first radiometric ages from the Judith River Formation (Upper Cretaceous), Hill County, Montana. Canadian Journal of Earth Sciences 26, 1384–1391.

Gradstein, F.M., Ogg, J.G., Smith, A.G., Bleeker, W., Lourens, L.J., 2004. A new Geologic Time Scale, with special reference to Precambrian and Neogene. Episodes 27, 83–100.

Harlan, S.S., Mehnert, H.H., Snee, L.W., Sheriff, S., Schmidt, R.G., 1991. New $^{40}Ar/^{39}Ar$ isotopic dates from the Adel Mountains Volcanics: Implications for the relationship between deformation and magnetism in the Montana Disturbed Belt, western Montana. Abstracts with Programs. Geological Society of America 23, 136.

Hicks, J.F., Obradovich, J.D., Tauxe, L., 1995. A new calibration point for the Late Cretaceous time scale: The $^{40}Ar/^{39}Ar$ isotopic age of the C33r/C33n geomagnetic reversal from the Judith River Formation (Upper Cretaceous), Elk Basin, Wyoming, USA. Journal of Geology 103, 243–356.

Hicks, J.F., Obradovich, J.D., Tauxe, L., 1999. Magnetostratigraphy, isotopic age calibration and intercontinental correlation of the Red Bird section of the Pierre Shale, Niobrara County, Wyoming, USA. Cretaceous Research 20, 1–27.

Horner, J.R., Schmitt, J.G., Jackson, F., Hanna, R., 2001. Bones and rocks of the Upper Cretaceous Two Medicine-Judith River clastic wedge complex, Montana. Museum of the Rockies Occasional Paper No. 3, 3–13.

Horner, J.R., Varricchio, D.J., Goodwin, M.B., 1992. Marine transgressions and the evolution of Cretaceous dinosaurs. Nature 358, 59–61.

Huff, W.D., 1983. Correlation of Middle Ordovician K-bentonites based on chemical fingerprinting. Journal of Geology 91, 657–669.

Huff, W.D., Kolata, D.R., 1989. Correlation of K-bentonite beds by chemical fingerprinting using multivariate statistics. In: Cross, T.A. (Ed.), Quantitative Dynamic Stratigraphy. Prentice Hall, Englewood Cliffs, New Jersey, pp. 567–577.

Jack, R.N., and Carmichael, I.S.E., 1969. The chemical 'fingerprinting' of acid volcanic rocks. California Division of Mines and Geology, Short Contributions 100, 17–32.

King, J.T., 1997. Facies analysis of the volcaniclastic Two Medicine Formation, Wolf Creek, Montana. Unpublished M.Sc. thesis, Department of Geology, The University of Montana, Missoula, Montana, 54 pp.

Klecka, W.R., 1981. Discriminant Analysis. In: Nie, N.H., Hull, C.H., Jenkins, J.G., Steinbrenner, K., Bent, D.H. (Eds.), SPSS: Statistical Package for the Social Sciences, second ed. McGraw-Hill, New York, pp. 434–467.

Kolata, D.R., Frost, J.K., and Huff, W.D., 1986. K-bentonites of the Ordovician Decorah Subgroup, upper Mississippi Valley: Correlation by chemical fingerprinting: Illinois State Geological Survey Circular 537, 30.

Lerbekmo, J.F., 1968. Chemical and modal analyses of some Upper Cretaceous and Paleocene bentonites from western Alberta. Canadian Journal of Earth Sciences 5, 1505–1511.

Lorenz, J.C., 1981. Sedimentary and tectonic history of the Two Medicine Formation, Late Cretaceous (Campanian), northwestern Montana. Unpublished Ph.D. thesis, Department of Geology, Princeton University, Princeton, New Jersey, 215 pp.

Lyons, J.B., 1944. Igneous rocks of the northern Big Belt range, Montana. Geological Society of America Bulletin 55, 445–472.

McLean, J.R., 1971. Stratigraphy of the Upper Cretaceous Judith River Formation in the Canadian Great Plains. Saskatchewan Research Council, Geology Division, Report 11, 96 pp.

Pellenard, P., Deconinick, J.-F., Huff, W.D., Thierry, J., Marchand, D., Fortwengler, D., Trouiller, A., 2003. Characterization and correlation of Upper Jurassic (Oxfordian) bentonite deposits in the Paris Basin and the Subalpine Basin, France. Sedimentology 50, 1035–1060.

Randle, K., Goles, G.G., Kittleman, L.R., 1971. Geochemical and petrological characterization of ash samples from Cascade Range Volcanoes. Quaternary Research 1, 261–282.

Renne, P.R., Swisher, C.C., Deino, A.L., Karner, D.B., Owens, T.L., DePaolo, D.J., 1998. Intercalibration of standards, absolute ages and uncertainties in $^{40}Ar/^{39}Ar$ dating. Chemical Geology 145, 117–152.

Roberts, E.M., 1999. A stratigraphic and sedimentologic analysis of the southern Two Medicine Formation, central Montana. Unpublished M.Sc. thesis, Department of Geology, University of Montana, Missoula, Montana, 80 pp.

Roberts, E.M., Hendrix, M.S., 2000. Taphonomy of a petrified forest in the Two Medicine Formation (Campanian), Northwest Montana: Implications for palinspastic restoration of the Boulder Batholith and Elkhorn Mountains Volcanics. Palaios 15, 478–482.

Roberts, E.M., Deino, A.L., Chan, M.A., 2005. $^{40}Ar/^{39}Ar$ age of the Kaiparowits Formation, southern Utah, and correlation of contemporaneous Campanian strata and vertebrate faunas along the margin of the Western Interior Basin. Cretaceous Research 26, 307–318.

Rogers, R.R., 1990. Taphonomy of three dinosaur bone beds in the Upper Cretaceous Two Medicine Formation of northwestern Montana: Evidence for drought-related mortality. Palaios 5, 394–413.

Rogers, R.R., 1994. Nature and origin of through-going discontinuities in nonmarine foreland basin strata, Upper Cretaceous, Montana: Implications for sequence analysis. Geology 22, 1119–1122.

Rogers, R.R., 1995. Sequence stratigraphy and vertebrate taphonomy of the Upper Cretaceous Two Medicine and Judith River formations, Montana. Unpublished Ph.D. thesis, Department of Geology, University of Chicago, Chicago, Illinois, 400 pp.

Rogers, R.R., 1998. Sequence analysis of the Upper Cretaceous Two Medicine and Judith River Formations, Montana: Nonmarine response to the Claggett and Bearpaw Marine Cycles. Journal of Sedimentary Research 68, 615–631.

Rogers, R.R., Swisher III, C.C., Horner, J.R., 1993. $^{40}Ar/^{39}Ar$ age and correlation of the nonmarine Two Medicine Formation (Upper Cretaceous), northwestern Montana, U.S.A. Canadian Journal of Earth Science 30, 1066–1075.

Ross, C.P., Andrews, D.A., and Witkind, I.J., 1955. Geologic map of Montana. United States Geological Survey, Map MR-411.

Russell, L.S., 1970. Correlation of the Upper Cretaceous Montana Group between southern Alberta and Montana. Canadian Journal of Earth Sciences 7, 1099–1108.

Sanderson, J.O.G., 1931. Upper Cretaceous volcanic ash beds in Alberta. Proceedings and Transactions of the Royal Society of Canada 25, 61–70.

Smedes, H.W., 1966. Geology and igneous petrology of the northern Elkhorn Mountains Jefferson and Broadwater counties, Montana. United States Geological Survey, Professional Paper 510, 116.

Smith, A.E. 1998. Volcanism and associated sedimentation in a retroarc foreland basin: the Upper Cretaceous Two Medicine Formation of west-central Montana. Unpublished M.Sc. thesis, Department of Geology, Montana State University, Bozeman, Montana, 170 pp.

Smith, A.E., Schmitt, J.G., 1998. Response of fluvial systems to explosive and effusive volcanism: Upper Cretaceous Two Medicine Formation, west-central Montana. Abstracts with Programs. Geological Society of America 30, 192.

Spivey, R.C. 1940. Bentonite in southwestern South Dakota. South Dakota Geological Survey, Report of Investigations 36, 56

Stebinger, E., 1914. The Montana Group of northwestern Montana. United States Geological Survey, Professional Paper 90-G, pp. 60–68.

Thomas, R.G., Eberth, D.A., Deino, A.L., Robinson, D., 1990. Composition, radioisotopic ages, and potential significance of an altered volcanic ash (bentonite) from the Upper Cretaceous Judith River Formation, Dinosaur Provincial Park, southern Alberta, Canada. Cretaceous Research 11, 125–162.

Tilling, R.I., Klepper, M.R., Obradovich, J.D., 1968. Potassium-argon ages and time of emplacement of the Boulder batholith, Montana. American Journal of Science 266, 671–689.

Vervoort, J.D., Wirth, K., Kennedy, B., Sandland, T., Harpp, K.S. The magmatic evolution of the Midcontinental rift: New geochronologic and geochemical evidence from felsic magmatism. Precambrian Research, in press. doi:10.1016/j.precamres.2007.02.019.

Viele, G.W., Harris II, F.G., 1965. Montana Group stratigraphy, Lewis and Clark County, Montana. American Association of Petroleum Geologists Bulletin 49, 379–417.

Winchester, J.A., Floyd, P.A., 1977. Geochemical discrimination of different magma series and their differentiation products using immobile elements. Chemical Geology 20, 325–343.

Wray, D.S., 1999. Identification and long-range correlation of bentonites in Turonian-Coniacian (Upper Cretaceous) chalks of northwest Europe. Geological Magazine 136, 361–371.